Sine-Gordon and Bose-Hubbard dynamics with photons in a hollow-core fiber

Ming-Xia Huo[1] and Dimitris G. Angelakis[1,2,*]

[1]*Centre for Quantum Technologies, National University of Singapore, 3 Science Drive 2, Singapore 117543, Singapore*

[2]*Science Department, Technical University of Crete, Chania, Crete GR-73100, Greece*

(Received 23 April 2011; published 17 February 2012)

We show that sine-Gordon and Bose-Hubbard dynamics with stationary polaritons could be observed in a hollow-core one-dimensional fiber loaded with a cold atomic gas. Utilizing the strong light confinement in the fiber, a range of different strongly correlated polaritonic and photonic states corresponding to both strong and weak interactions can be created and probed. The key ingredient is the creation of a tunable effective lattice potential acting on the interacting polaritonic gas, which is possible by slightly modulating the atomic density. We analyze the relevant phase diagram corresponding to the realizable Bose-Hubbard (weak) and sine-Gordon (strong) interacting regimes and conclude by describing the measurement process. The latter consists of mapping the stationary excitations to propagating light pulses whose correlations can be efficiently probed once they exit the fiber using available optical technologies.

DOI: 10.1103/PhysRevA.85.023821 PACS number(s): 42.50.Gy, 71.10.Pm

I. INTRODUCTION

The Bose-Hubbard (BH) and sine-Gordon (sG) models have been extremely successful in describing a range of quantum many-body effects and especially quantum phase transitions (QPT) [1]. Cold atoms in optical lattices so far have been the most famous platform to implement these models, where the Mott insulator (MI) to superfluid (SF) QPT for a weakly interacting gas in a deep lattice potential was observed [2]. More recently, it became possible to tune the interactions between the atoms in the gas, leading to the realization of the sG model and the Pinning QPT [3,4].

Alternative platforms in the field of quantum simulations of many-body effects involve ions for quantum magnets [5] and more recently photonic lattices for the understanding of in-equilibrium and out-of-equilibrium quantum many-body effects [6]. The photon-based ideas are motivated by significant advances in the fields of cavity QED and quantum nonlinear optics [7] and have initiated a stream of works on the many-body properties of both closed and lossy cavity arrays [8]. More recently, a new direction has appeared in the field of strongly correlated photons where hollow-core optical fibers filled with cold atomic gases were considered [9,10]. The strong light confinement and the resulting large optical nonlinearities in the single-photon level predicted for similar systems [11] have motivated new proposals to observe photon crystallization and photonic spin-charge separation [12].

We show here that it is possible to impose an effective *lattice potential* on the strongly interacting polaritonic gas in the fiber. This opens up possibilities for a large range of Hamiltonians to be simulated with photons. Our first examples analyze the simulation of the sG and BH models. We show that the whole-phase diagram of the Mott-to-SF transitions for both models can be reproduced, including a corresponding photonic "pinning transition." We conclude with a discussion on the available tunability of the quantum optical parameters for the observation of the strongly correlated phases. The latter is possible by releasing the trapped polaritons and measuring the correlation on the photons emitted at the other end of the fiber using available optical technology.

II. MODEL SETUP

The considered atomic level structure is shown in Fig. 1 and comprises the typical stationary light setup [7,11] of Λ type atoms interacting with a probe and a control field. The process to steer the system to the relevant strongly correlated regimes can be divided into four stages: preparation and loading, steering to strong interactions, creation of effective polaritonic lattice, and measurement or probing of the phase diagram. In the first stage, the one-dimensional cold atomic ensemble is prepared outside the fiber using standard cold atom techniques and is then transferred in the hollow core as described in [10]. The atoms are initially in the ground state $|a\rangle$, and the fiber is injected with a quantum coherent pulse $\hat{E}_+$ and a classical field Ω_+ from the left side. Switching off the control field allows for the storage of the quantum pulse in the medium in the usual slow-light manner. In the second stage, a pair of classical fields $\Omega_\pm$ are subsequently switched on from both sides [Fig. 1(b)], making the stored excitation quasistationary [11]. During this part, the initially detuned fourth level is adiabatically brought closer to resonance, allowing for the required nonlinear interactions. At this stage, the dynamics of the polaritons are described by a nonlinear Schrödinger equation as analyzed in [12] and can be tuned to either a strongly or a weakly interacting regime. As we show here, an effective periodic potential can be imposed on the polariton gas by slightly periodic modulating the atomic density, which allows for the simulation of a range of many-body effects on a lattice like the pinning transition.

At the end of the second stage, the dynamics of photons inside the medium is governed by the quantum nonlinear Schrödinger equation [11,12]:

$$i\partial_t \Psi = -\frac{1}{2m}\partial_z^2 \Psi + V\Psi + 2\chi \Psi^\dagger \Psi^2. \quad (1)$$

Here $\Psi = (\Psi_+ + \Psi_-)/2$ is a dark-state quasistationary polariton trapped in the Bragg grating created by the standing wave formed by the control fields $\Omega_\pm = \Omega$. $\Psi_\pm$ are the forward- and

*dimitris.angelakis@gmail.org

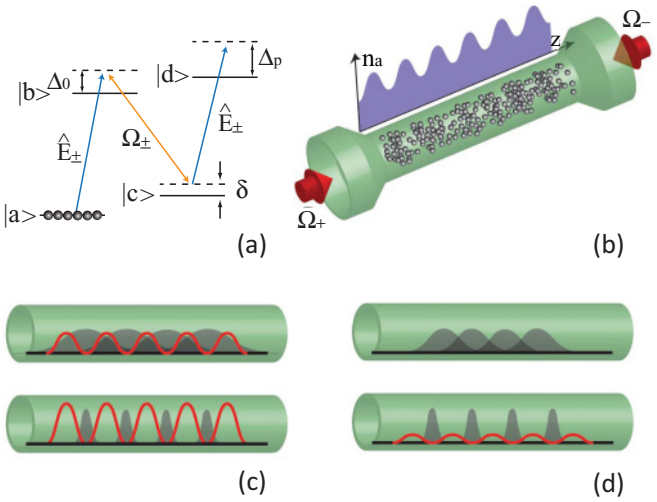

FIG. 1. (Color online) In panels (a) and (b), an ensemble of cold atoms with a four-level structure interacts with a pair of classical fields $\Omega_\pm$ in the hollow core. The fields create an effective Bragg grating that transforms the excitations carried by an input pulse E_+ into a quasistationary strongly interacting polariton gas [gray areas in panels (c) and (d)]. By modulating the density of the cold atomic ensemble, an effective tunable lattice potential for the polaritons can be created, shown by red lines in panels (c) and (d). The interactions of the trapped polariton gas and the depth of the effective lattice can be tuned to simulate the BH or sG many-body dynamics and probe the corresponding quantum phase transition from SF (upper part) to MI (lower part) in panels (c) and (d). By switching Ω_- off, the photons exit the fiber and the phases of the system can be probed by performing standard optical measurements, evaluating the first- and second-order coherence functions of the emitted light.

backward-propagating polaritons originating from the coupled photonic fields $\hat{E}_\pm$ to atomic spin-wave excitations. In the limit of a large optical depth,[1] the symmetric combination Ψ survives the time evolution while the antisymmetric combination $A = (\Psi_+ - \Psi_-)/2$ is adiabatically eliminated. The presence of one-photon detuning Δ_0 leads to a quadratic dispersion for the polariton field where the effective mass is $m = -\frac{\Delta\omega}{2v v_g} - \frac{\Gamma_{1D} n_a}{4\Delta_0 v_g}$; v and $v_g \simeq \frac{v\Omega^2}{\pi g^2 n_a}$ are the group velocities of light in empty and doped fibers, respectively. $\Delta\omega$ is the difference between the frequencies of quantum and classical fields, $\omega_q - \omega_c$, and Γ_{1D} is the spontaneous emission into the fiber modes. The presence of δ (energy shift of level $|c\rangle$; Fig. 1) and Δ_p (single photon detuning from the fourth level) leads to the potential and interaction terms given as $V = \frac{\Delta\omega v_g}{v} - \frac{\Lambda\Gamma_{1D}\delta v_g n_a}{4\Omega^2}$ and $\chi = \frac{\Lambda^2\Xi\Gamma_{1D}v_g}{2\Delta_p}$, where $\Lambda = \frac{\Omega^2}{\Omega^2 - \delta\Delta_0/2}$ and $\Xi = \frac{\Delta_p - \delta/2}{\Delta_p - \delta}$.

III. ADDING A PERIODIC POTENTIAL

We add an effective polaritonic lattice by inducing a periodic atomic density distribution through the application of an external field such that the atoms in $|a\rangle$ are now given by $n_a = n_0 + n_1 \cos^2(\pi n_{\rm ph} z)$. Applying a microwave field at state $|a\rangle$ as a standing wave resonant with another hyperfine state $|u\rangle$ will transfer atoms from $|a\rangle$ to $|u\rangle$, depending on their position in the field envelope. The ones on the nodes will not be affected, and the ones on the antinodes will be most affected. The final percentage of atoms "carved" off the initial homogenous density will depend on the interaction time. Note that $|u\rangle$ state is not involved in the electromagnetically induced transparency process. Assuming we tuned the interaction time such that $n_0 \gg n_1$, the new Hamiltonian reads

$$H = \int dz \Psi^\dagger \left[\frac{\hbar^2}{2m}\nabla^2 + V_0 + V_1 \cos^2(\pi n_{\rm ph} z) \right] \Psi + \chi \int dz \Psi^\dagger \Psi^\dagger \Psi \Psi, \tag{2}$$

where by tuning $\Delta\omega$ and δ, V_0 is zero and $V_1 = -\Lambda\Gamma_{1D}\delta v_g n_1/(4\Omega^2)$ is the resulting imposed polaritonic lattice depth. We stress here the dependance of the effective polaritonic lattice on both the slow light parameters (group velocity, trapping laser detuning and strength) and the modulated atomic density. Finally, we note that the atomic lattice modulation should be commensurate with the number of the photons in the initial pulse for the pinning transition to occur [4]. This means that the modulation length will approximately fall in the microwave regime as the numbers of trapped photons in the initial pulse are of the order of ten and the fiber is a few centimeters in length.

IV. REACHING THE RELEVANT CORRELATED REGIMES

The degree of achieving a specific strongly correlated polaritonic-photonic state is characterized by the feasibility of tuning the Lieb-Liniger ratio of the interaction and kinetic energies γ and the ratio of the depth of the polaritonic potential to the recoil energy V_1/E_R to the relevant regimes [1,2]. With $E_R = \pi^2 n_{\rm ph}^2/2m$ in our system, the above quantities read

$$\gamma = \frac{m\chi}{n_{\rm ph}} = -\frac{\Lambda^2\Xi}{8}\frac{\Gamma_{1D}^2}{\Delta_0\Delta_p}\frac{n_0}{n_{\rm ph}}, \tag{3}$$

$$\frac{V_1}{E_R} = \frac{\Lambda}{8\pi^2}\frac{\Gamma_{1D}^2}{\Omega^2}\frac{\delta}{\Delta_0}\frac{n_0 n_1}{n_{\rm ph}^2}. \tag{4}$$

Both can be controlled by tuning the one-photon detuning Δ_p/Γ (shifting the fourth level $|d\rangle$ to or from the resonance), by changing the strength of the control laser Rabi frequency Ω, and by tuning the atomic density modulation n_1/n_a. In Fig. 2(a), we plot the achievable regimes for γ as a function of $\Delta_p/\Gamma, \Omega/\Gamma$. In Fig. 2(b), we plot V_1/E_R as a function of Ω/Γ and n_1/n_a. We assume a total atomic decay rate from the upper level $\Gamma \simeq 20$ MHz, approximately atomic density of $n_a = 10^7$ m^{-1} (10^5 atoms into a 1-cm-long fiber), and a photonic density of $n_{\rm ph} = 10^3$ m^{-1} (with the input quantum light pulse containing roughly 10 photons). For these values, γ and V_1/E_R can be tuned in the range 0 to 5 and 0 to 30 respectively, which allows for both the strong and weak interaction regimes to be realized with our trapped polaritonic gas. We note that the current state of the art in the number of atoms loaded in similar hollow-core fibers is smaller by roughly one order of

[1] OD $= n_a L\Gamma_{1D}/\Gamma$ and $\Gamma_{1D} = 4\pi g^2/v$ with Γ/Γ_{1D} being the ratio of the total spontaneous emission rate to spontaneous emission into the waveguide.

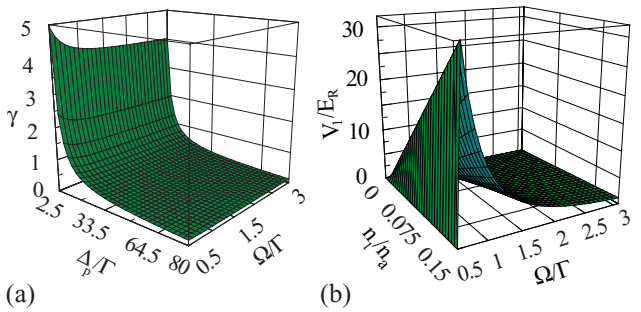

FIG. 2. (Color online) Plots of the Lieb-Liniger interaction parameter γ as a function of the one-photon detuning Δ_p/Γ and the Rabi frequency Ω/Γ of the classical laser field (a) and the lattice depth V_1/E_R as a function of Ω/Γ and the atomic density perturbation n_1/n_a (b). The parameters are taken as $n_a = 10^7\mathrm{m}^{-1}$, $n_{\mathrm{ph}} = 10^3\mathrm{m}^{-1}$, and $\Gamma_{1D} = 0.2\Gamma$, $\Delta_0 = 5\Gamma$, and $\delta = 0.01\Gamma$ with $\Gamma \simeq 20$ MHz as the atomic decay rate.

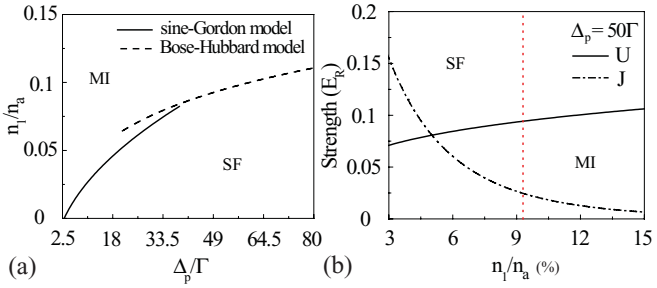

FIG. 3. (Color online) (a) The phase diagram for the trapped polaritons in the fiber as a function of the single-photon detuning and the atomic modulation, Δ_p/Γ and n_1/n_a, for the case of $\Omega = \Gamma$. (b) The interaction and tunneling strength for the weakly interacting gas in the BH regime. The red dotted line at $n_1/n_a \simeq 0.093$ corresponds to the Mott phase transition point $(U/J)_c \simeq 3.85$. The rest of the parameters are as in Fig. 2.

magnitude or less. However, recent experimental progress in the field shows that our requirements should be satisfied in the very near future [10].

The losses, which mainly occur due to spontaneous emission from the upper levels, can be estimated by including the corresponding terms in the Hamiltonian Eq. (2). In that case, the effective parameters acquire an imaginary part which for the effective mass, for example, reads $m = -\Delta\omega/(2vv_g) - \Gamma_{1D}n_a/(4\Delta_0 v_g + 2i\Gamma v_g)$, leading to a loss rate of $\kappa = \frac{n_{\mathrm{ph}}^2 v_g \Gamma}{n_a \Gamma_{1D}}$. These losses set an upper bound on the time scales for the preparation of the states and the probing of the established correlations. For the values under consideration in our system (see Fig. 2), these translate to time scales of a few milliseconds, which are within the reach of current optical loading and measurement technology.

V. POLARITONIC-PHOTONIC PINNING TRANSITION

We now discuss the nature of the many-body states generated by the addition of the effective polaritonic potential and show that a "pinning transition" for polaritons can be observed, similar to the one recently experimentally verified for bosonic atoms [4]. This polaritonic pinning transition is expected to transform continuously into the BH regime for sufficiently deep effective lattices (large V_1/E_R) and small interactions γ. To analyze each relevant phase of the system, we make use of the corresponding BH and sG models from many-body physics [1]. We also discuss the feasibility of accessing the whole of the relevant phase diagram for both cases, by simply tuning the optical parameters in our system.

We first analyze the strong interaction regime $1 \leqslant \gamma \leqslant 5$ for a weak effective potential, $V_1/E_R \leqslant 3$. This regime is clearly accessible in our photonic system, as we show in Fig. 2, by appropriate tuning of the one-photon detuning Δ_p, the control laser strength Ω, and the periodic distributed atomic density n_1. In this case, the proper low-energy description of the system described in Eq. (2) is given by the quantum sG model, which reads [1]

$$H = \int \frac{dz}{2}\left\{\frac{\hbar v_g}{\pi}[(\partial_z\theta)^2 + (\partial_z\phi)^2] + V_1 n_{\mathrm{ph}}\cos(4K\theta)\right\}. \quad (5)$$

The first two terms account for the kinetic and interaction energies of polaritons respectively, and $\partial_z\theta$ and $\partial_z\phi$ denote the fluctuations of the long-wavelength density and phase fields θ and ϕ [1]. The dimensionless parameter $K = \hbar n_{\mathrm{ph}}\pi/(mv_g)$ is known to be related to γ as $K \simeq \pi/\sqrt{\gamma - \gamma^{3/2}/(2\pi)}$ for $\gamma \leqslant 10$.

On the other hand, if we tune the system to the weak interaction limit with small $\gamma \leqslant 1$ and large V_1/E_R with $V_1/E_R \gg 1$, the system is characterized in a good approximation by the BH model [2],

$$H = -J\sum_i (b_i^\dagger b_{i+1} + \mathrm{H.c.}) + \frac{U}{2}\sum_i n_i(n_i - 1), \quad (6)$$

where $J/E_R = 4(V_1/E_R)^{3/4}\exp(-2\sqrt{V_1/E_R})/\sqrt{\pi}$, $U/E_R = \sqrt{2/\pi^3}(V_1/E_R)^{1/4}\gamma$.

In Fig. 3(a), we show that by simply varying Δ_p/Γ and n_1/n_a, the whole phase diagram corresponding both to the sG and BH regimes can be accessed in our system for realistic values of the optical parameters. We plot the known phase-transition lines corresponding to the sG and BH model occurring at $V_1/E_R = 2\pi/\sqrt{\gamma - \gamma^{3/2}/(2\pi)} - 4$ and $(U/J)_c = \sqrt{2}\exp(2\sqrt{V_1/E_R})\gamma/[4\pi(V_1/E_R)^{1/2}] \simeq 3.85$, respectively [1,2]. In our case, these are probed by adjusting the detuning and the laser coupling accordingly. The pinning transition from SF to Mott is expected to occur for small single-photon detunings $\Delta_p/\Gamma \leqslant 20$ and for any atomic density modulation n_1/n_a less than 5% which correspond to $\gamma \geqslant 3.5$. The BH Mott transition will occur in the opposite weakly interacting regime and deeper lattices. In Fig. 3(b), for a specific value of the $\Delta_p/\Gamma = 50$ corresponding to the system with $\gamma \ll 1$, we plot the interaction U and tunneling J strengths as a function of n_1/n_a to illustrate the BH dynamics. We see that the transition occurs for $n_1/n_a \simeq 0.093$, which corresponds to known critical point of $(U/J)_c \simeq 3.85$.

We mention here that our approach is adiabatic so the initial input coherent state, an eigenstate of the initial noninteracting Hamiltonian, will always remain an eigenstate of the instantaneous Hamiltonian and no dynamics or intermediate phases will show up. This can be seen as follows: For the first part, the preparation of the strongly interacting polariton gas is achieved by slowly increasing γ from an initial small value $\gamma \ll 1$ as

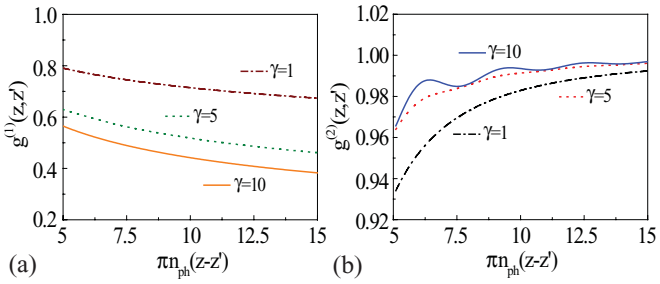

FIG. 4. (Color online) The correlation functions $g^{(1)}$ and $g^{(2)}$ for the trapped polariton gas in the strongly interacting regime (sG model) as a function of the distance for different values of the interaction strength γ for vanishing potential depth. The shown behavior is directly mapped to the first and the second coherence functions of the photons exiting the fiber, which can be measured using standard optical techniques. Note the emergence of oscillation in $g^{(2)}$ as the system gets closer to the Tonks gas.

$\gamma = \gamma_0 e^{\omega_F t}$ with $\omega_F \sim n_{\rm ph}^2/m$ the effective Fermi energy in the center of the pulse. The t is estimated to be smaller than the polariton dynamics in this case (see analysis in Chang *et al*. [12]). For the second part of the process, we adiabatically ramp up the polariton lattice by slowly modulating the atomic density as $n_1 = (n_1)_0 e^{\beta t}$. The latter approach, followed in cold-atom physics as well [13], ensures that keeping $U/\beta \gg 1$ is enough to secure a slow sweep. In our case, as we need to shift $(n_1)_0 = 0.01 n_a$ to $n_1 = 0.1 n_a$—and correspondingly $U_0 = 0.06 E_R$ to $U = 0.1 E_R$—across the phase diagram in Fig. 3(b), the above condition translates into an adiabatic operation time of milliseconds. The latter is smaller than the reported polariton storage times of seconds [14].

VI. MEASUREMENT

Once the system is driven to the desired regime by tuning γ and $V_1/E_{\rm R}$, one of the control fields, say Ω_-, is switched off, mapping the quasistationary polaritons to propagating photons and releasing the excitations [11]. Any spatial correlations of the polaritonic states will be mapped to temporal ones on the outgoing photons, which can be probed using standard photodetection measurements. The momentum distribution can be easily constructed by a measurement on the first-order coherence function $g^{(1)}(z,z') = \langle \hat{E}(z)\hat{E}^\dagger(z')\rangle$ and then taking the Fourier transform [2]. We note here the *in situ* character of such a measurement in this optical setup is in contrast to the usual release and time-of-flight measurement required in the cold-atom setups. In addition, second-order coherence measurements on the outgoing photons can be easily made, revealing the density-density correlations of the states prepared in the fiber. For the case of the system being in the strong interaction regime, for example, with a zero lattice potential as a Luttinger liquid, the first- and second-order correlations are known and to leading order are [1] $g^{(1)} \sim 1/(z-z')^{2K}$ and $g^{(2)} = \frac{\langle n(z)n(z')\rangle}{\langle n(z)\rangle\langle n(z')\rangle} \simeq n^2 + \frac{cK}{(z-z')^2} + \frac{c'\cos(2\pi n(z-z'))}{(z-z')^{2K}}$ with $n = \langle \hat{E}(z)\hat{E}^\dagger(z)\rangle$, where K as function of γ is given earlier and c, c' are constants. We plot these correlations in Fig. 4 for three different values of γ corresponding to states close to the horizontal axis of the phase diagram in Fig. 3(a). For small but finite polariton lattice depths and $\gamma \gg 1$ (left-hand corner of phase diagram), the photons will be pinned. The correlations then will exhibit the characteristic behavior of insulating states with strong antibunching appearing in the $g^{(2)}$ measurements at distances inversely proportional to the photon density in the fiber (not shown here). Finally, for the right-hand side, the phase diagram in Fig. 3(a) (SF part in the BH model), the general solutions are not known but the usual power law decay is expected in $g^{(1)}$ accompanied by the relevant bunching of the photons in $g^{(2)}$.

VII. CONCLUSION

In conclusion, we have shown that different strongly correlated states of photons could be created inside hollow-core fibers interacting with atomic gases with current or near-future optical technology. The resulting states can be controllably tuned to reproduce sG and BH many-body dynamics and also used to probe the corresponding pinning quantum phase transition predicted by these models. The various correlated phases can be analyzed by standard optical correlations measurements on the light exiting the fiber.

ACKNOWLEDGMENTS

We acknowledge useful discussions with L. C. Kwek and K. S. Huang in the early stages of this work and the financial support by the National Research Foundation and Ministry of Education, Singapore.

[1] S. Sachdev, *Quantum Phase Transitions* (Cambridge University Press, Cambridge, UK, 1999); T. Giamarchi, *Quantum Physics in One Dimension* (Oxford University Press, Oxford, 2004).

[2] D. Jaksch, C. Bruder, J. I. Cirac, C. W. Gardiner, and P. Zoller, Phys. Rev. Lett. **81**, 3108 (1998); M. Greiner, O. Mandel, T. Esslinger, T. W. Hansch, and I. Bloch, Nature (London) **415**, 39 (2002).

[3] H. P. Büchler, G. Blatter, and W. Zwerger, Phys. Rev. Lett. **90**, 130401 (2003).

[4] E. Haller, R. Hart, M. J. Mark, J. G. Danzl, L. Reichsöllner, M. Gustavsson, M. Dalmonte, G. Pupillo, and H.-C. Nägerl, Nature (London) **466**, 597 (2010).

[5] A. Friedenauer, H. Schmitz, J. T. Glueckert, D. Porras, and T. Schaetz, Nat. Phys. **4**, 757 (2008).

[6] D. G. Angelakis, M. F. Santos, and S. Bose, Phys. Rev. A **76**, 031805(R) (2007); M. J. Hartmann, F. G. S. L. Brandão, and M. B. Plenio, Nat. Phys. **2**, 849 (2006); A. D. Greentree, C. Tahan, J. H. Cole, and L. C. L. Hollenberg, Nat. Phys. **2**, 856 (2006).

[7] H. Walther, B. T. H. Varcoe, B.-G. Englert, and T. Becker, Rep. Prog. Phys. **69**, 1325 (2006); M. Fleischhauer, A. Imamoglu, and J. P. Marangos, Rev. Mod. Phys. **77**, 633 (2005).

[8] D. Rossini and R. Fazio, Phys. Rev. Lett. **99**, 186401 (2007); N. Na, S. Utsunomiya, L. Tian, and

Y. Yamamoto, Phys. Rev. A **77**, 031803(R) (2008); M. Aichhorn, M. Hohenadler, C. Tahan, and P. B. Littlewood, Phys. Rev. Lett. **100**, 216401 (2008); D. Gerace, H. E. Türeci, A. Imamoglu, V. Giovannetti, and R. Fazio, Nat. Phys. **5**, 281 (2009); I. Carusotto, D. Gerace, H. E. Tureci, S. DeLiberato, C. Ciuti, and A. Imamoglu, Phys. Rev. Lett. **103**, 033601 (2009); D. G. Angelakis, S. Bose, and S. Mancini, Europhys. Lett. **85**, 20007 (2009); M. Kiffner and M. J. Hartmann, Phys. Rev. A **82**, 033813 (2010).

[9] S. Ghosh, J. E. Sharping, D. G. Ouzounov, and A. L. Gaeta, Phys. Rev. Lett. **94**, 093902 (2005); K. P. Nayak, P. N. Melentiev, M. Morinaga, F. L. Kien, V. I. Balykin, and K. Hakuta, Opt. Express **15**, 5431 (2007); T. Takekoshi and R. J. Knize, Phys. Rev. Lett. **98**, 210404 (2007).

[10] C. A. Christensen, S. Will, M. Saba, G. B. Jo, Y. I. Shin, W. Ketterle, and D. Pritchard, Phys. Rev. A **78**, 033429 (2008); S. Vorrath, S. A. Möller, P. Windpassinger, K. Bongs, and K. Sengstock, New J. Phys. **12**, 123015 (2010); M. Bajcsy, S. Hofferberth, T. Peyronel, V. Balic, Q. Liang, A. S. Zibrov, V. Vuletic, and M. D. Lukin, Phys. Rev. A **83**, 063830 (2011).

[11] M. D. Lukin and A. Imamoglu, Phys. Rev. Lett. **84**, 1419 (2000); M. Fleischhauer and M. D. Lukin, *ibid*. **84**, 5094 (2000); M. Bajcsy, A. S. Zibrov, and M. D. Lukin, Nature (London) **426**, 638 (2003); M. Bajcsy, S. Hofferberth, V. Balic, T. Peyronel, M. Hafezi, A. S. Zibrov, V. Vuletic, and M. D. Lukin, Phys. Rev. Lett. **102**, 203902 (2009); E. Shahmoon, G. Kurizki, M. Fleischhauer, and D. Petrosyan, Phys. Rev. A **83**, 033806 (2011); Kiffner and M. J. Hartmann, *ibid*. **81**, 021806(R) (2010).

[12] D. E. Chang, V. Gritsev, G. Morigi, V. Vuletic, M. D. Lukin, and E. A. Demler, Nat. Phys. **4**, 884 (2008); D. G. Angelakis, M. Huo, E. Kyoseva, and L. C. Kwek, Phys. Rev. Lett. **106**, 153601 (2011).

[13] R. Schützhold, M. Uhlmann, Y. Xu, and U. R. Fischer, Phys. Rev. Lett. **97**, 200601 (2006).

[14] R. Zhang, S. R. Garner, and L. V. Hau, Phys. Rev. Lett. **103**, 233602 (2009); U. Schnorrberger, J. D. Thompson, S. Trotzky, R. Pugatch, N. Davidson, S. Kuhr, and I. Bloch, *ibid*. **103**, 033303 (2009).